www.ietdl.org

Published in IET Microwaves, Antennas & Propagation
Received on 26th February 2014
Revised on 20th April 2014
Accepted on 22nd May 2014
doi: 10.1049/iet-map.2014.0121

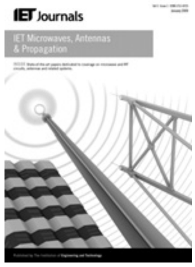

ISSN 1751-8725

Substrate integrated waveguide antenna subarray for broadband circularly polarised radiation

Tarek Djerafi[1,2], Bassel Youzkatli-el-Khatib[2], Ke Wu[2], Serioja-Ovidiu Tatu[1]

[1]Énergie Matériaux et Télécommunications, Institut National de la Recherche Scientifique, Montréal, QC, Canada H5A 1K6
[2]Poly-Grames Research Center, École Polytechnique de Montréal, Montréal, QC, Canada H3C 3A7
E-mail: djerafi@emt.inrs.ca

Abstract: This study presents a compact circularly polarised array using tapered slot antenna fed by a substrate integrated waveguide (SIW) power divider. With the proposed topology, broadband circularly polarised property is achieved and total gain can be increased by controlling the element length, conserving the same footprint area. The different 2 × 2 cell configurations are investigated. Simple and integrated series–parallel SIW feed for the choose cell is presented. A 2 × 2 antenna array is designed and fabricated using SIW *E*-plane power divider. The measured 10 dB return loss and 3 dB axial ratio bandwidths are 35.65 and 32.3%, respectively. The measured antenna gain is 14.4 dBi at 35 GHz.

1 Introduction

The circular polarisation (CP) is indispensable in wireless communication, radar and imaging systems [1–3]. The antenna in those system designs have to accomplish required gain to compensate for the high path loss at millimetre wave bands. A simple antenna element gain can be enhanced per different methods as: ring-shaped dielectric resonator [4] or mushroom-like structure [5] use. Since the gain is generally not sufficient, an appropriate antenna array must be configured as in [6–10].

A compact sequential-phase (SP) microstrip feed for circularly polarised sequential-rotation 2 × 2 patch array is presented in [6], achieving 5% of bandwidth with maximum gain of 7.5 dBi. Simple and compact shorted loop structure is used as feeding of 2 × 2 single-fed corner-truncated patch array [7], the AR bandwidth has been improved to 7% with peak gain of 10.5 dBi. Travelling wave excitation of cavity-backed aperture antenna is presented in [8]. In this design, 2 × 2 array shows the 3 dB axial ratio (AR) bandwidth about 50% and half-power gain bandwidth about 40% about 10 GHz. Substrate integrated waveguide (SIW)-based CP array antennas are proposed in [9, 10], taking the advantage of field shielding, low cost and weight. In [9], a 2 × 2 and 2 × 4 arrays at X-band (from 8.0 to 8.5 GHz) with a right hand circular polarisation characteristic is developed. Four-way and eight-way power dividers ensure progressive phase shift for sequential feeding [9]. Respectively, gains of 10.9 and 14.3 dBi are realised with 7.2 and 6.6% of AR bandwidths. In [10], a 4 × 4 antenna array is designed and fabricated using low- temperature cofired ceramic technology at 60 GHz. A metal-topped via fence is introduced around the strip to reduce the mutual coupling between the array elements. The measured results show that the AR bandwidth is more than 7 GHz and gain is about 17.5 dBi.

To accommodate the polarising components, the CP element array requires an additional layer of circuitry, which increases fabrication cost and complexity. In addition, at high frequency, polariser circuits show high ohmic loss, thereby reducing the overall efficiency of the array. The CP elements are typically broadside radiating elements as patches, printed dipoles and slots. Generally, the used elements are resonant structures and yield narrow bandwidth and low gain. Another method to increase an array AR bandwidth is to use the sequential rotation feeding technique. In fact, it is possible to generate CP radiation by using properly phased rotating linearly polarised (LP) elements [11, 12]. When LP array element is used, the design process of the array antenna (with sequential rotation technique) will be easier than that for the CP array element type. This is because the process of adjusting the CP performance of each array element can be avoided. However, the resulting compound array gain is 3 dB lower than the array using the CP element [11, 12].

This paper introduces a novel SIW array, based on linear tapered-slot antennas (TSAs) and sequential rotation to ensure the CP performance in wide bandwidth and to achieve higher gain performances. The antenna element is presented as well as feed structure. An analysis of different configurations, based on the proposed element and the feeding network, is presented. A 2 × 2 element array is fabricated and the experimental data are displayed.

2 Design procedure and fabrication

This section will investigate the single antenna. This element can then be integrated into a subarray cell to determine the optimal geometry. The substrate RT/Duroid 6002 with thickness b of 508 μm and dielectric constant ε_r of 2.94 is

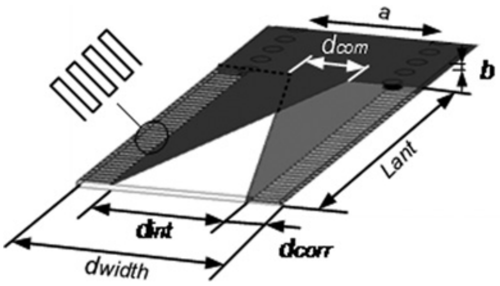

Fig. 1 *Corrugated ALTSA fed by SIW structure and microstrip to SIW transition*

selected for this application. The antenna was designed in Ansoft high-frequency structure simulator (HFSS) to operate in the Kα-band.

2.1 Antenna element

The element is an antipodal linear tapered slot end-fire antenna with corrugations as shown in Fig. 1. The corrugation length d_{corr} is selected to be around $\lambda_r/4$ (λ_r is the wavelength in the dielectric substrate) [13]. This corrugation is proposed for effectively reducing the antenna width d_{width} without degrading the antenna radiation performance. The choice of SIW feeding avoids the balanced to unbalanced transformer ('Balun') requirement. The optimised antenna dimensions are listed in Table 1.

Table 1 Dimensions of the corrugated antipodal LTSA (mm)

Parameters	a	d_{corr}	d_{comm}	d_{width}	L_{ant}
	4.6	1.14	3.04	7.8	16.6

Simulated results are obtained by applying a full wave analysis under HFSS. It can be noted that the antenna bandwidth covers the entire considered frequency band from 26.5 to 40 GHz. With L_{ant} of 16.6 mm equivalent to three λ_r, the gain of a single element starts from 9.8 dBi at 26.5 GHz to 11.9 dBi at 40 GHz. The cross-polarisation level with corrugations is found to be better than 22 dB at 26.5 GHz and 17 dB at 40 GHz. To realise the desired gain, antenna length L_{ant} can be increased to reach the value of eight λ_r and obtain typical values about 17 dB for long elements [14].

2.2 Unit cell configuration

The four elements are physically rotated relative to each other and the feed phase is individually adjusted for each arrangement as shown in Fig. 2. The first basic subarray has its elements arranged in a 2 × 2 square or rectangular grid configuration as shown in Fig. 2*a*. The feed phases are arranged in either a 0, 90, 0 and 90° or a 0, 90, 180 and 270° [15]. In the second configuration, two elements in 90° configuration duplicated in parallel define a 2 V shape as shown in Fig. 2*b*. In this second case, the suitable feed

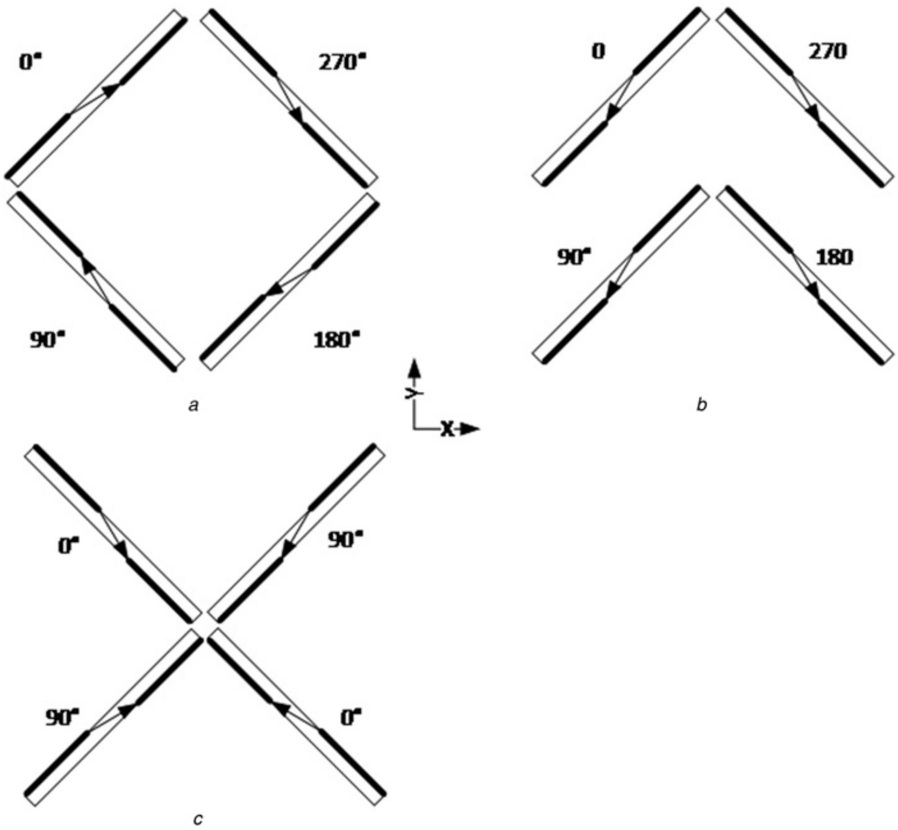

Fig. 2 *Array configurations of sequentially rotated TSA (with linear polarisation excitation line)*

a Cell1: square configuration
b Cell2: V configuration
c Cell3: X configuration

doi: 10.1049/iet-map.2014.0121

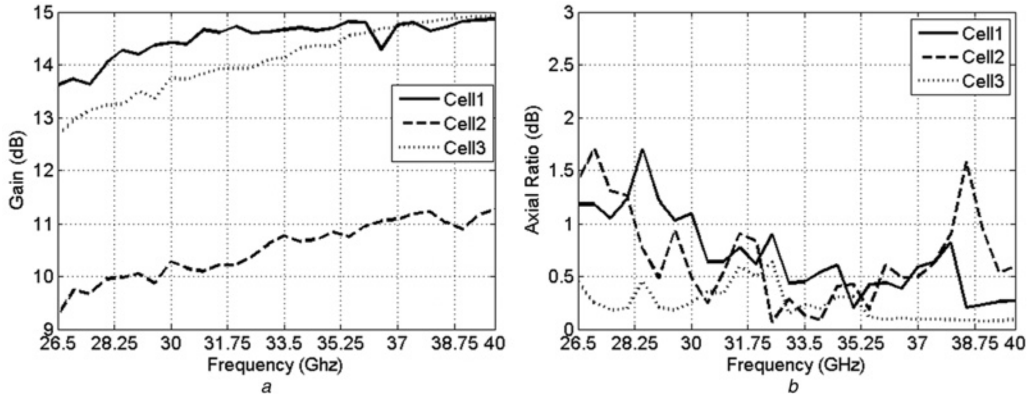

Fig. 3 *Simulated performance of the three proposed configurations illustrated in Fig. 2*

a Gain
b AR

phase distributions which give the better result is 0, 90, 0 and 90° or 0, 270, 90 and 180°. In the third configuration, the elements are arranged in X with feed phases of 0, 90, 0 and 90° as shown in Fig. 2*c*. The distances between the elements in the three cases are: $\Delta x = 6$ mm and $\Delta y = 6.35$ mm equivalent to 0.7 λ_0 and 0.74 λ_0, respectively. Additional 180° in two diagonal elements change the CP from RH to LH and vice versa. Any of these elements can be rotated physically by 180° with adequate phase compensation.

The gain and AR of the three configurations are presented in Figs. 3*a* and *b*, respectively. The three configurations show good simulated AR in the whole bandwidth. This is because of the chose phase feed, in these arrangements the co-pols are reinforced but the cross-pols cancel. As can be concluded from the excitation line illustrated in Fig. 2, for example in the square configuration, most of the radiation impurities from the 0° element cancels that from the 180° element, and likewise for the 90 and 270° elements.

The gain of an element inserted in the array is generally smaller because of the mutual coupling. In fact, the four times duplication with in phase feed can increase the single element gain by 6 dB to get in touch with 18 dBi. Rotating LP elements' array becomes 50% less aperture efficient than a CP elements' array (when element distance is $>0.7\lambda_0$ [11]). This reduction of the gain by 3 dB is observed in the case of the first and third cells where the maximum gain achieves 15 dBi.

Fig. 4 illustrates in the field distribution in the transverse view when just one port is excited. The mutual coupling effect change with configuration, the first cell shows better gain performance. As seen in Fig. 4*b*, this coupling is very high between two elements disposed in the parallel arrangement as in V configuration and directly affects the centre of the element 2. The total gain is in the same level of one element. The third case is the complement of the first one to build larger antenna array. The field distribution in the three cases gives idea about the expected asymmetrical radiation pattern.

2.3 Array topologies

Since a number of years, different TSA arrays have been proposed, studied and developed using the third dimension. Vivaldi is used in [16] to build planar array, in one plane the antenna is integrated with microstrip feeding and in the other plane connectors and wiring are necessary. In [17], dual polarisation cell in X configuration is proposed. In those two designs, extra components are needed between the element and the feed limiting the integration.

The most significant advantage of SIW technology is the possibility to integrate all the components on the same

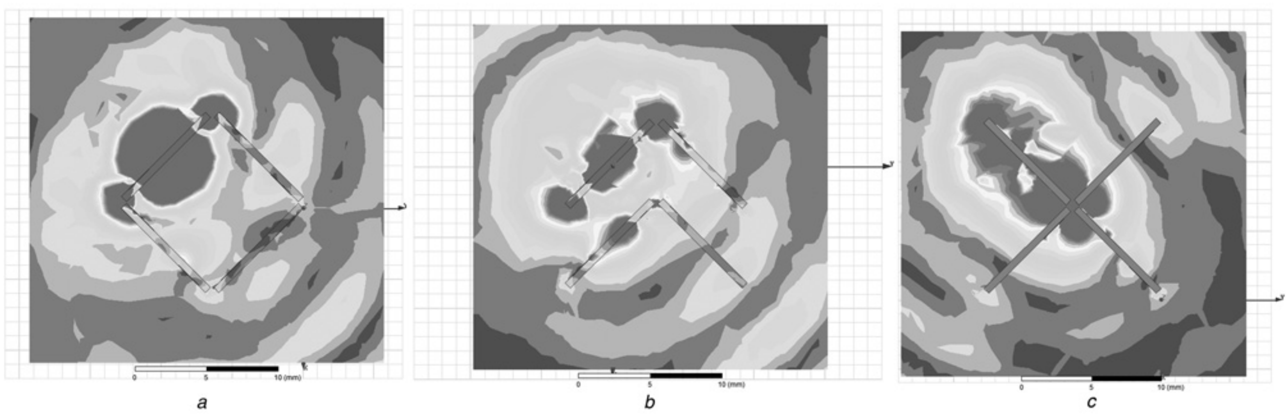

Fig. 4 *Simulated E-field magnitude distributions obtained by HFSS in transverse cut*

a Case1: square configuration
b Case2: V configuration
c Case3: X configuration

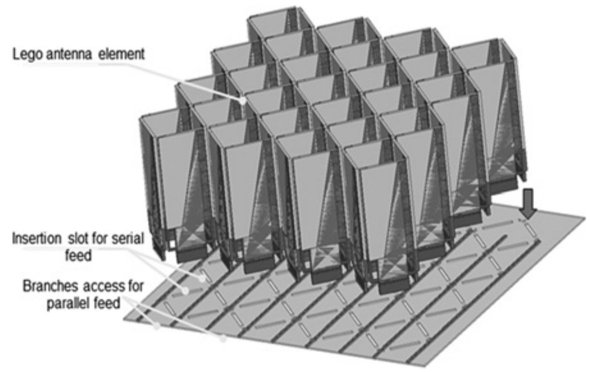

Fig. 5 *Illustrative LEGO-style design of an antenna array system: 8 × 8 elements array (4 × 4 cells) with integrated feed*

substrate, including passive components and even antennas. Different antenna feeds and beamforming networks have been extensively studied and demonstrated with the SIW schemes and promising results have been already obtained [18].

A 1/16 *H*-plane parallel power divider is designed to produce a low sidelobe level with amplitude distribution across the array aperture [19]. Eight 1 × 8 are inserted at the end of the 16 branches thanks to *H*-to-*E* plan corner. To realise the corner, a vertical line is inserted into a horizontal line. The vertical line is terminated by a non-metalised section having the width of the equivalent waveguide and the length equal to the horizontal line substrate thickness [20]. This power divider is used to feed the designed corrugated Fermi-TSA.

The proposed design combines serial and parallel feeds as shown in Fig. 5. To feed 4 × 4 cells, eight parallel branches with eight slots disposed in series should be used. The insertion slots are used to integrate the vertical antenna, and to avoid the coaxial connecters, as used in conventional solutions.

2.4 Feeding network

The first configuration (Fig. 2*a*) is selected to be built, in order to demonstrate the subarray capabilities. The *E*-plane rectangular waveguide corner is very useful in

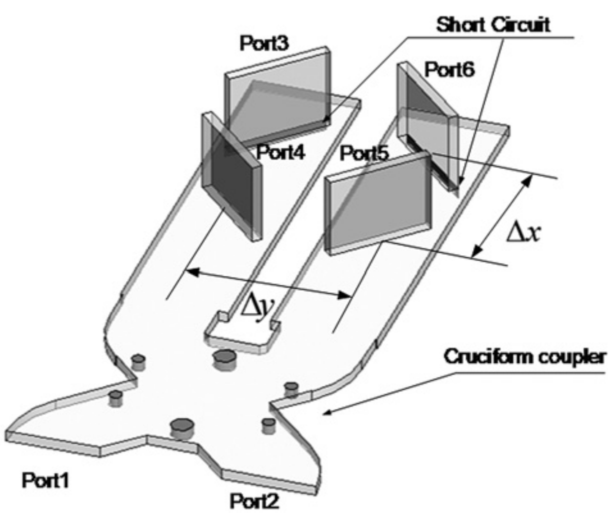

Fig. 6 *Feeding network for the rectangulaire cellulle: cruciform SIW coupler feed the two branches, two vertical lines are inserted in each of the two branches*

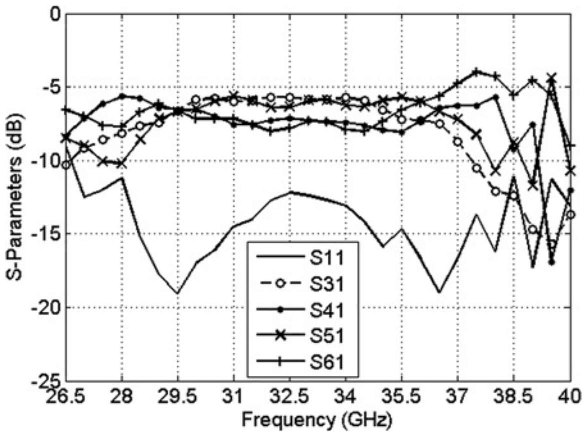

Fig. 7 *Simulated S-parameters of the feeding network*

multi-polarisation antenna feeding. To feed the small cell of 2 × 2 elements, two branches are needed with two slots disposed in series with 90° of delay. Two vertical waveguides with adequate distance are used to construct the *E*-plane feeding structure needed for one branch. The final distances between the elements are Δx = 7 mm and Δy = 7.25 mm equivalent to 0.77 λ_0 and 0.8 (considered at 33 GHz λ_0), respectively. The second stage of the vertical lines has to be short circuited as shown in Fig. 6.

To ensure 90° of phase difference between the two branches excitation, a wideband coupler is added. SIW *H*-plane cruciform directional coupler topology was selected as it is well adapted for planar realisations [21]. A 3.25 ± 0.25 dB of power imbalance with matching and isolation levels better than 20 dB is observed over the

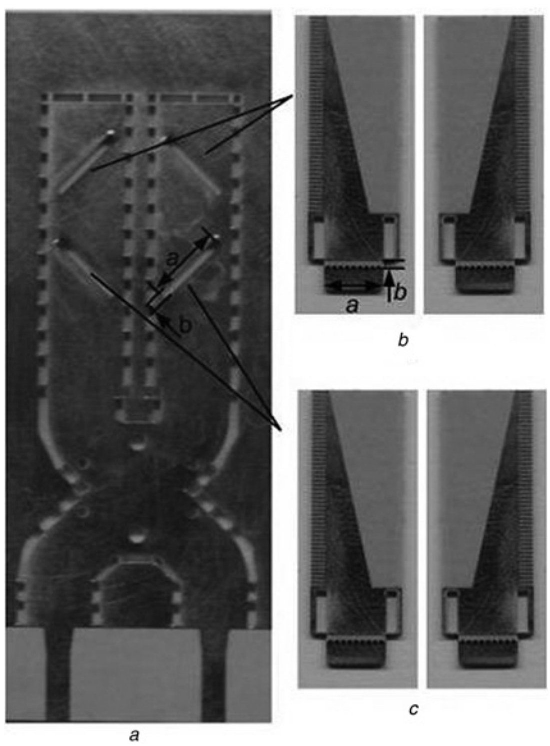

Fig. 8 *Layout of the different parts used to construct the antenna before assembling*

a Feeder with coupler and the four slots
b Vertical line with linear TSA for the back elements (top and bottom)
c Vertical line with linear TSA for the front elements (top and bottom)

doi: 10.1049/iet-map.2014.0121

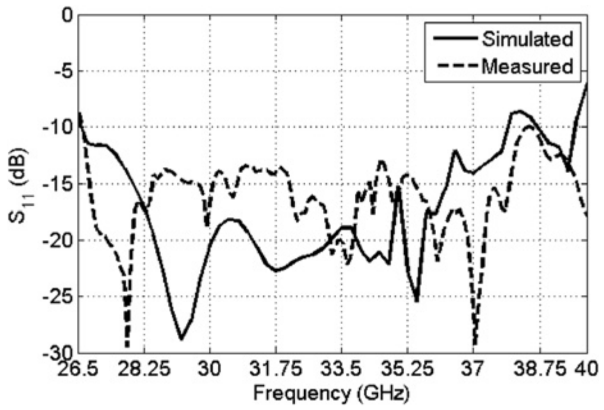

Fig. 9 *Simulated and measured return losses of the antenna array*

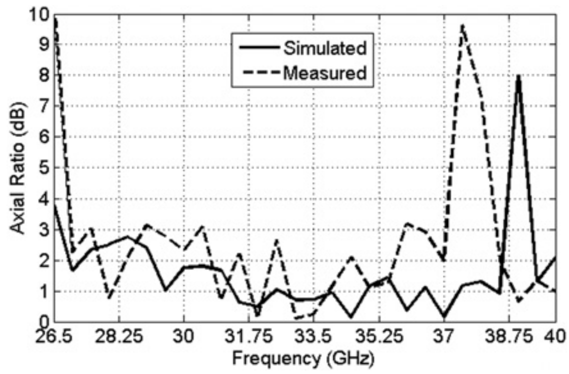

Fig. 11 *Simulated and measured AR of the antenna array*

frequency range represents a 28% relative bandwidth, which is appropriate to our wideband applications. Port 1 of the cruciform coupler is used to achieve the required phase.

Fig. 7 shows that the input power is uniformly divided into the SP-feed ports, namely Port 3 to Port 6. The measured balance bandwidth for the ±1 dB balance level ranges from 28.5 to 37 GHz, about 26%. The maximum imbalance and return loss appears about 38.5 GHz, in fact higher-order modes appear in the vertical section region. Compared with needed phase arrangement (0, 90, 0 and 90°), we generate (0, 90, 0 and −90°). To overcome this problem, the antipodal linearly TSA (ALTSA) feed by the Port 6 will be rotated by 180° compensating the phase error.

2.5 Fabrication

The array is developed with different fabricated parts: the waveguide feeder and the antennas as shown in Fig. 8. The different parts are assembled like LEGO elements to construct the array. The vertical elements with antenna and SIW line are inserted into the feeding network (Fig. 9*a*). In this feeder, four slots are created with the width of the vertical line substrate thickness (*b*) and the length (*a*) equal to the vertical line equivalent waveguide width. The vertical elements are terminated by a non-metalised section having the width of the equivalent waveguide the substrate thickness (*b*). This non-metalised section is present on the two sides of the forward-facing elements (Fig. 9*b*). In the back elements, the non-metalised slot is etched just in front, the reverse present total short circuit (Fig. 9*c*).

3 Experimental results

Fig. 9 presents the simulated and measured matching results for the four-element TSA subarray feed by Port 1. It is seen that the measured 10 dB return loss bandwidth is 35.65% of the centre frequency 33.5 GHz. The slight difference between simulated and measured results is attributed to the manual assemblage.

Radiation pattern measurement is made in an MI (2000) Technology anechoïde room in Poly-Grames Research Center. The Port 1 is fed when second port is loaded. The gain with the horizontal and vertical polarisations instead of the gain aligned with the major and minor axes of the polarisation ellipse are measured. A simulated far-field radiation pattern at the centre operating frequency is shown in Fig. 10*a*. It can be seen that the patterns are quite symmetric with respect to the normal to the antenna surface; the gain is about 14.4 dBi and side lobe levels are lower than 14 dB. The 3 dB beam widths in the two planes are almost the same.

The measurement shows good agreement with the simulation (Fig. 10) with minor discrepancies in symmetry and SLL levels. This could be because of the visual alignment in the anechoïde chamber which explains difference in gain in the two planes. The measured gain ~0.5 dB lower than the simulated, this loss is caused by the dielectric loss and metal conductivity. In fact, the simulated result just dielectric loss is considered without the metallic loss and used loss tangent is underestimated (specified by the fabricant at low frequency).

Fig. 11 presents the comparison of measured and simulated AR results of the circularly polarised slot subarray. It is seen

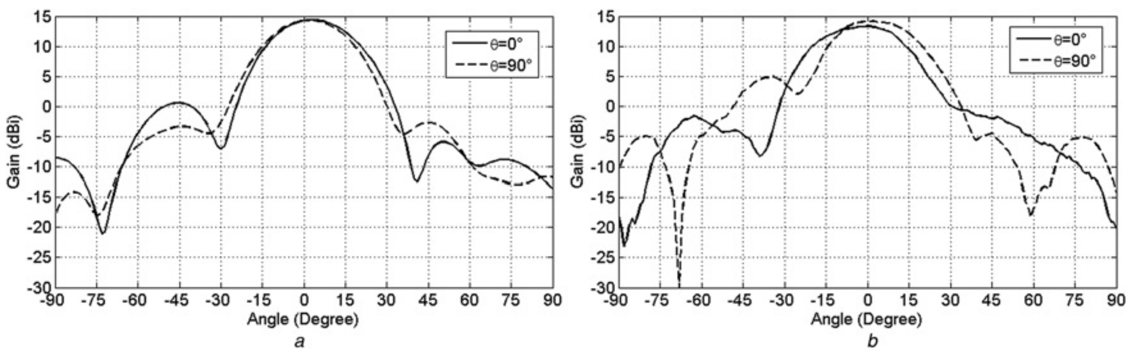

Fig. 10 *Far-field radiation patterns in YZ (θ = 0°) and XZ (θ = 90°) planes at 35 GHz*

a Simulated
b Measured

doi: 10.1049/iet-map.2014.0121

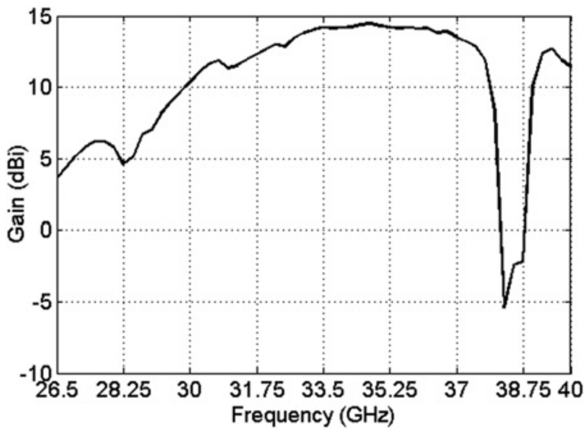

Fig. 12 *Measured gains of the antenna array*

that the frequency range for 3 dB AR is from 26.7 to 37 GHz, which equals to 32.3% of the centre frequency. The simulated result achieves 2 GHz wider bandwidth and lower AR. The measured performance degradation has also the origin probably on the visual alignment of the antenna. Compared with the result shown in Fig. 3, the feed network add reduces the AR bandwidth and level performances.

Fig. 12 shows the measured gain of the proposed 2 × 2 antenna array. In the band of 33–37 GHz, the gain variation is <1 dB. The half-power gain bandwidth is from 30.5 to 38 GHz (22%). In this bandwidth, the array satisfies the 10 dB return loss, the 3 dB AR and the half-power gain performances at the same time which are still wideband numbers. In this bandwidth, the radiation efficiency is 85% in simulation (without the conductor loss) and 72% in the measurement. The drop on the gain about 38 GHz is because of the relatively poor feeding network *S*-parameters at this frequency, as illustrated in Fig. 7. The AR and gain are more sensible to the power and phase equalities of the power divider which reduce the bandwidth.

Table 2 compares the performances of the presented design with the LC SIW array works presented in references [9, 10]. The proposed antenna shows the wider impedance and AR bandwidths. The gain aperture efficiency of the proposed design is higher; the gain can be increased in the same area by increasing the antenna length L_{ant}. Thus, the proposed architecture promises to be a viable candidate for circularly polarised array applications.

The gain of each element can be increased by increasing the length. The gain of the simulated cell saturates at 17.2 dBi, which corresponds to L_{ant} of 45 mm. This structure is used as elements of a planar array, as illustrated in Fig. 5, where identical 4 × 4 cells are positioned in regular geometrical shape, with inter-element space of 13 mm in the two planes. Therefore the gain increases with 12 dB, to reach the impressive value of 29 dBi, without deterioration of the AR. In practice, to feed this array three 90° couplers combines are needed, which increase considerably the size. A multilayer structure can be used to eliminate this inconvenience.

Table 2 Comparison of the presented antenna with references

Structures	Frequencies, GHz	Area, λr_2	Gains, dBic	3 dB AR, %
2 × 2 [9]	8–8.5	4.5 × 4.5	10.9	7.2
2 × 4 [9]	8–8.5	4.5 × 4.5	14.3	6.6
4 × 4 [10]	60.2–67	7.9 × 7.9	17.5	10.7
2 × 2 this work	26.7–37	2.5 × 2.5	14.4	32.3

4 Conclusions

In this paper, a very compact circular polarised array based on end-fire structure and three-dimensional power divider is proposed. Constructed in SIW exclusively, the antenna system has the further advantage of small size and light weight. The AR bandwidth has been widened by adopting a rotated LP leaky wave antenna. To generate CP radiation, four linearly TSA are sequentially rotated. Four *H*-to-*E* interconnects with coupler are used to connect the feed network.

Simulation and experimental studies are performed, which show that the AR bandwidth and gain are directly proportional to disposition of the element. The measured impedance bandwidth of the antenna array is 35.65% with the return loss below 10 dB. The 3 dB AR bandwidth is 32.3%. Thus promises to be a viable candidate for circularly polarised array applications. It is interesting as future works to: (i) feed network performance should be optimised; (ii) reduce the distance between the elements using higher permittivity substrate; and (iii) design a larger array.

5 References

1 Shen, T., Kao, T., Huang, T., Tu, J., Lin, J., Wu, R.: ‘Antenna design of 60-GHz micro-radar system-in-package for noncontact vital sign detection’, *IEEE Antennas Wirel. Propag. Lett.*, 2013, **11**, pp. 1–4

2 Encheng, W., Zhuopeng, W., Zhang, C.A.: ‘Wideband antenna for global navigation satellite system with reduced multipath effect’, *IEEE Antennas Wirel. Propag. Lett.*, 2013, **12**, pp. 124–127

3 Longfang, Z., Fumeaux, C.E.: ‘A cross-shaped dielectric resonator antenna for multifunction and polarization diversity applications’, *IEEE Antennas Wirel. Propag. Lett.*, 2011, **10**, pp. 742–745

4 Perron, A., Denidni, T.A., Sebak, A.R.: ‘High-gain circularly polarized millimeter-wave antenna’. Antennas Propagation Society Int. Symp., Charleston, SC, 2009, pp. 1–4

5 Boutayeb, H., Djerafi, T., Wu, K.: ‘Gain enhancement of a circularly polarized microstrip patch antenna surrounded by a circular mushroom-like substrate’. European Wireless Technology Conf. (EuWIT), Paris, 2010, pp. 257–260

6 Lin, S-K., Lin, Y-C.: ‘A compact sequential-phase feed using uniform transmission lines for circularly polarized sequential-rotation arrays’, *IEEE Trans. Antennas Propag.*, 2011, **59**, (7), pp. 2721–2724

7 Li, Y., Zhang, Z., Feng, Z.: ‘A sequential-phase feed using a circularly polarized shorted loop structure’, *IEEE Trans. Antennas Propag.*, 2013, **61**, (3), pp. 1443–1447

8 Hung, K.-F., Lin, Y.-C.: ‘Novel broadband circularly polarized cavity-backed aperture antenna with traveling wave excitation’, *IEEE Trans. Antennas Propag.*, 2010, **58**, (1), pp. 35–42

9 Jung, E-Y., Lee, J.W., Lee, T.K., Lee, W-K.: ‘SIW-based array antennas with sequential feeding for X-band satellite communication’, *IEEE Trans. Antennas Propag.*, 2012, **60**, (8), pp. 3632–3639

10 Li, Y., Chen, Z.N., Qing, X., Zhang, Z., Xu, J., Feng, Z.: ‘Axial ratio bandwidth enhancement of 60-GHz substrate integrated waveguide-fed circularly polarized LTCC antenna array’, *IEEE Trans. Antennas Propag.*, 2012, **60**, (10), pp. 4619–4626

11 Hall, P.S., Dahele, J.S., James, J.R.: ‘Design principles of sequentially fed, wide bandwidth, circularly polarized microstrip antennas’, *IEE Proc.*, 1989, **136**, (5), pp. 381–389

12 Hall, P.S.: ‘Application of sequential feeding to wide bandwidth, circularly polarised microstrip patch arrays’, *IEE Proc.*, 1989, **136**, (5), pp. 390–398

13 Djerafi, T., Wu, K.: ‘Corrugated substrate integrated waveguide (SIW) antipodal linearly tapered slot antenna array fed by quasi-triangular power divider’, *Prog. Electromagn. Res. C*, 2012, **26**, pp. 139–151

14 Yngvesson, K.S., Korzeniowski, T.L., Kim, Y.S., Kollberg, E.L., Johansson, J.F.: ‘The tapered slot antenna – a new integrated element for millimeter-wave applications’, *IEEE Trans. Microw. Theory Tech.*, 1989, **37**, (2), pp. 365–374

15 Bhattacharyya, A.K.: 'Comparison between arrays of rotating linearly polarized elements and circularly polarized elements', *IEEE Trans. Antennas Propag.*, 2008, **56**, pp. 2949–2954
16 Yang, Y., Wang, Y., Fathy, A.E.: 'Design of compact Vivaldi antenna arrays for UWB see through wall applications', *Prog. Electromagn. Res.*, 2008, **82**, pp. 401–418
17 Sutinjo, A., Tung, E.: 'The design of a dual polarized Vivaldi array', *Microw. J.*, 2004, pp. 152–161
18 Wu, K., Cheng, Y.J., Djerafi, T., Hong, W.: 'Substrate-integrated millimeter-wave and terahertz antenna technology', *Proc. IEEE*, 2012, **100**, (7), pp. 2219–2232
19 Youzkatli el khatib, B., Djerafi, T., Wu, K.: 'Three dimensional architecture of substrate integrated waveguide feeder for Fermi tapered slot antenna array applications', *IEEE Trans. Antennas Propag.*, 2012, **60**, (10), pp. 4610–4618
20 Youzkatli El Khatib, B., Djerafi, T., Wu, K.: 'Substrate integrated waveguide vertical interconnects for three-dimensional integrated circuits', *Trans. Compon. Packag. Manuf. Technol.*, 2012, **2**, (9), pp. 1526–1535
21 Djerafi, T., Fonseca, N.J.G., Wu, K.: 'Design and implementation of a planar 4 × 4 butler matrix in SIW technology for wide band high power applications', *Prog. Electromagn. Res. B*, 2011, **35**, pp. 29–51